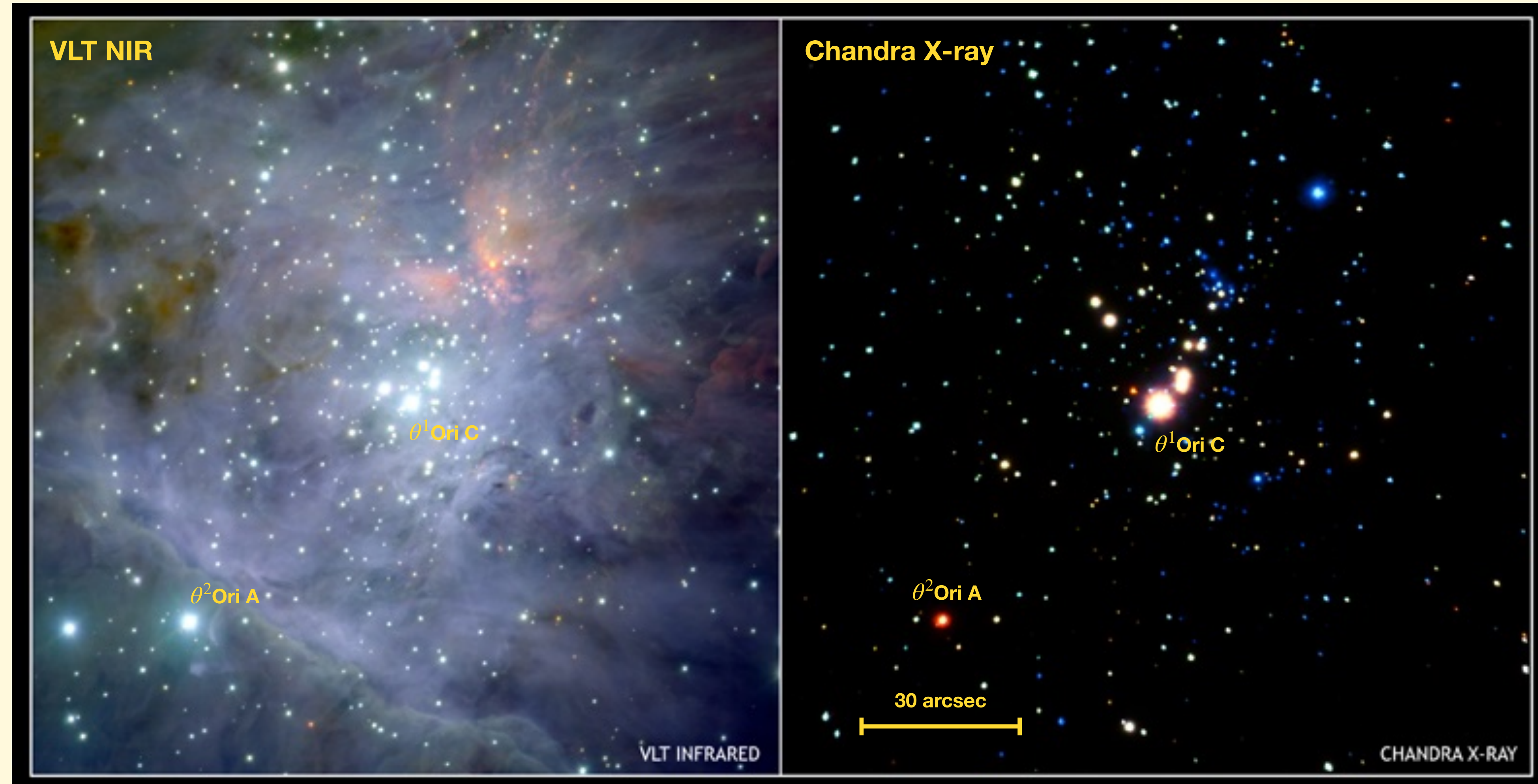


The Nature of X-rays from Young Stellar Objects in the Orion Nebula Cluster -A Chandra HETG Legacy Project-

By **Dave Principe** (MIT) on behalf of the ONC HETG Team: **Norbert S. Schulz** (MIT; Project PI), **David P. Huenemoerder** (MIT), Dave Principe (MIT), **Marc Gagne** (West Chester University), **Hans Moritz Günther** (MIT), **Joel Kastner** (RIT), **Joy Nichols** (Harvard CfA), **Andrew Pollock** (University of Sheffield), **Thomas Preibisch** (Universitäts-Sternwarte München), **Paola Testa** (Harvard CfA), **Fabio Reale** (University of Palermo), **Jun Yang** (MIT), and **Claude R. Canizares** (MIT)



The Orion Nebula Cluster is the nearest site of massive star formation. It includes more than a thousand young (< 5 Myr), protoplanetary disk-hosting stars and a handful of massive early-type zero-age main sequence stars. An 840 ks ACIS-I imaging campaign (Getman et al. 2005) characterized X-ray emission from ~1600 young star systems (lower right image).



Credit: ESO/VLT/M.McCaughrean et al.

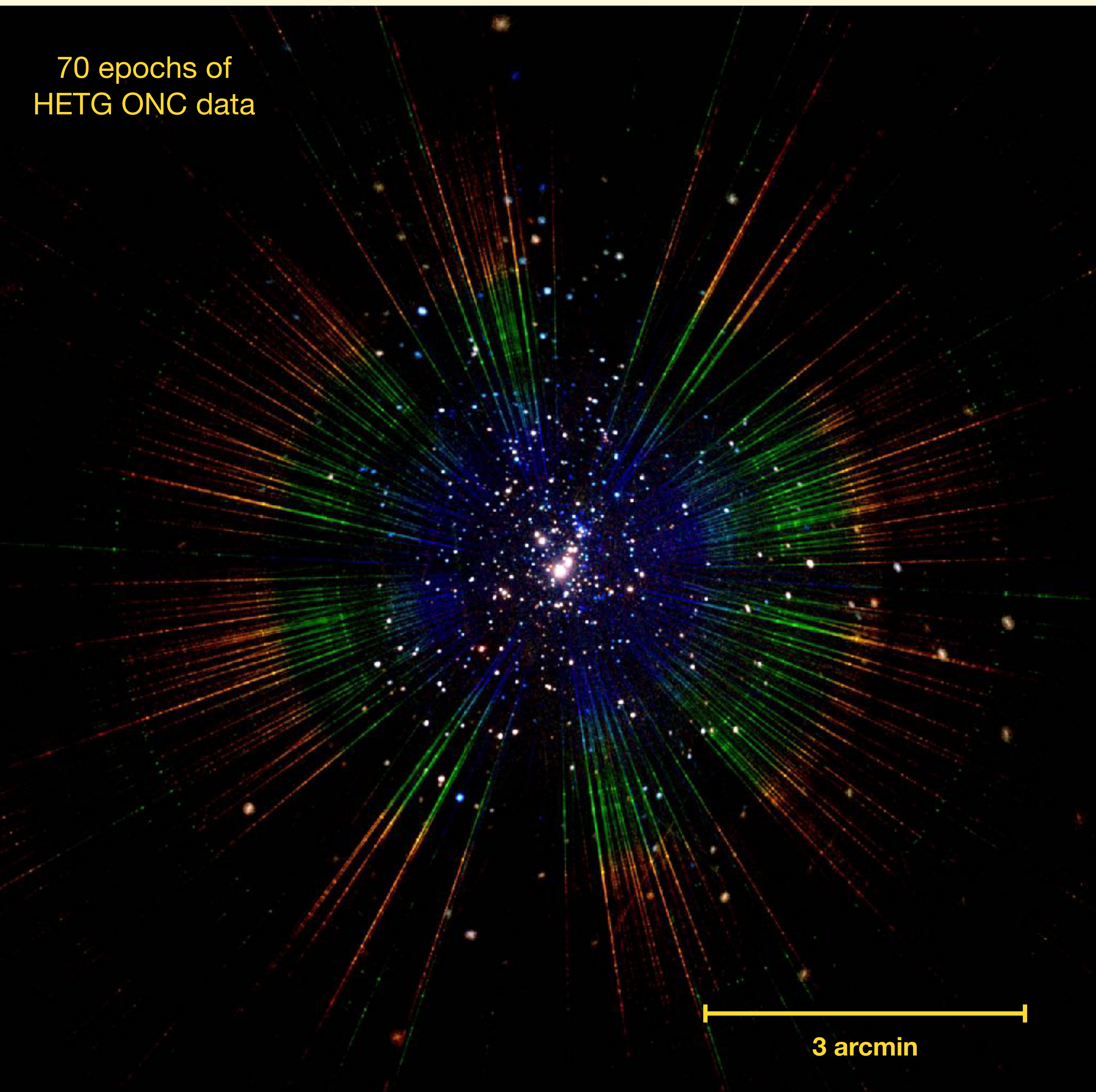
Credit: NASA/CXC/Penn State/E.Feigelson & K.Getman et al.

A Chandra HETG Legacy Project

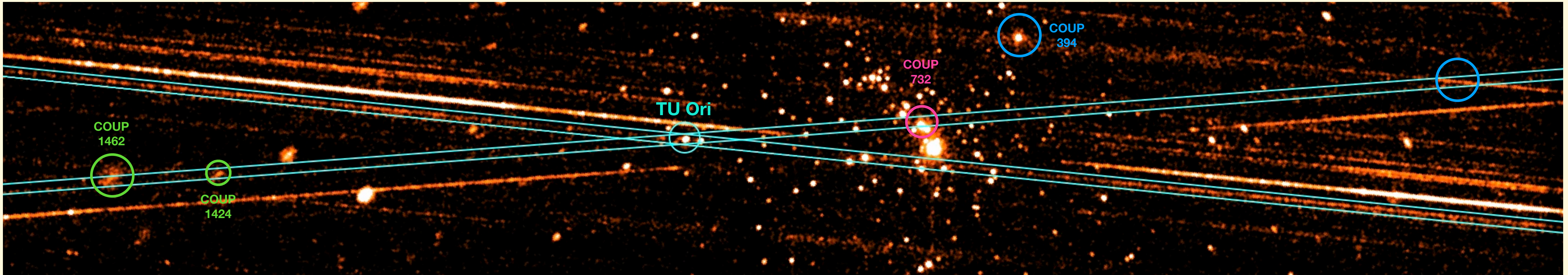
The ONC HETG project includes 70 observations taken over the lifetime of Chandra (1999-2020) spanning a total of ~2.1 megaseconds. The merged image of all 70 observations is shown (right).

The HETG instrument disperses light onto ACIS-S from every source in the field of view in a characteristic ‘X’ shape pattern. Since brighter sources disperse more events, the spectrum of the massive star θ^1 Ori C taken at multiple roll angles dominates this image. Colors represent X-ray energy from hard (blue) to soft (red).

At a distance of ~400 pc, the ONC represents the ideal crowded field target. It is close enough to provide enough counts for high resolution spectroscopy of stars and distant enough for many sources to fall near the telescope pointing where Chandra’s PSF is excellent.

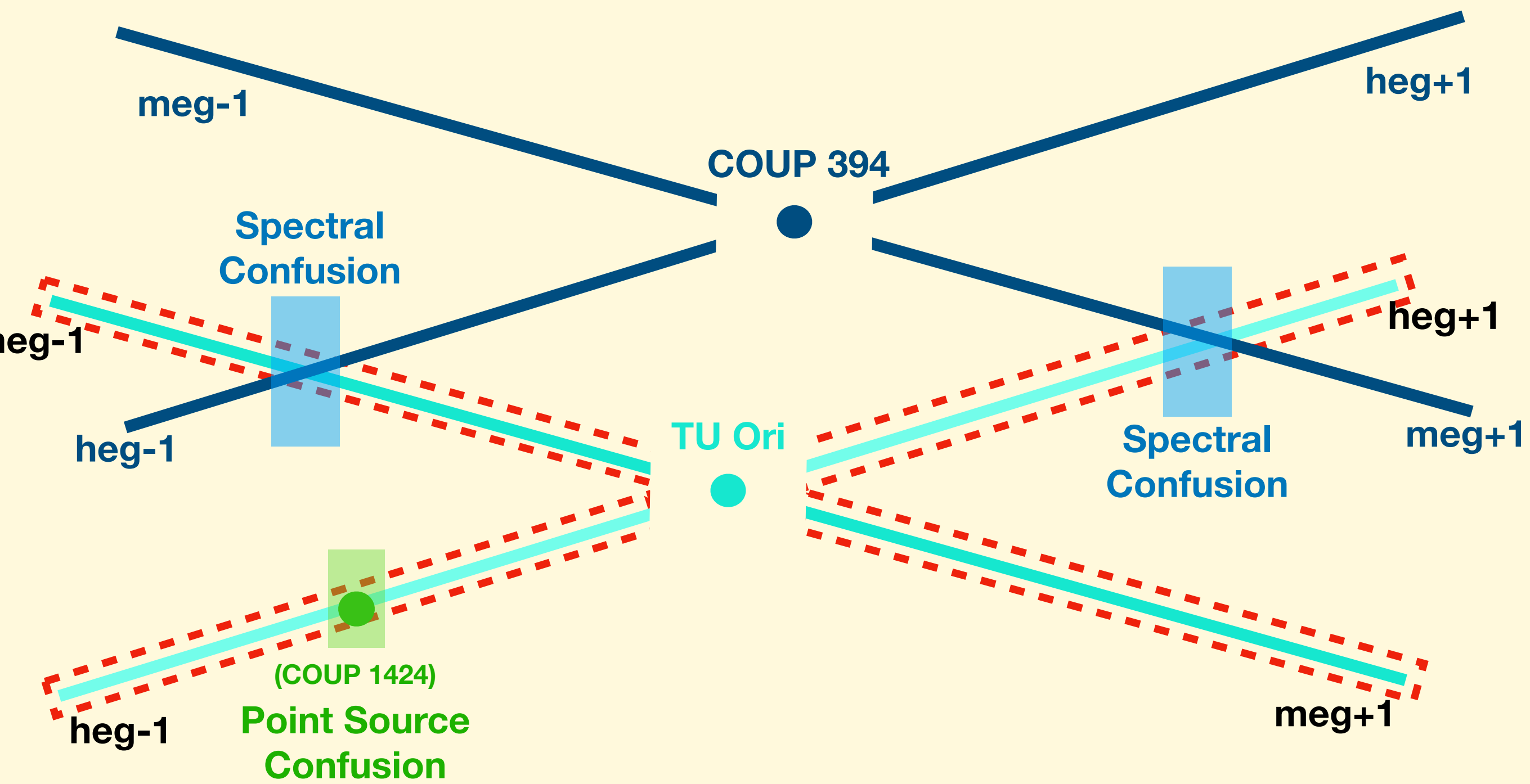


Accounting for Sources of Confusion in Each Extracted Spectrum



In a crowded field like the ONC, the dispersed spectra of individual source overlaps (intersects) with other sources in the field of view. These sources of confusion must be accounted for in each epoch when attempting to jointly fit all 70 epochs.

A specialized python routine called CrissCross has been developed as part this project and accounts for all sources of potential confusion. For each extracted spectrum, CrissCross identifies the wavelength (energy) where confusion occurs so these can be accounted for in spectral fitting.



Characterizing the Spectra of Emission Line Dominated Stars

θ^1 Ori C
O7V

Table 6. HETG Spectral Parameters of 2 Temperature APED fits:

Star	N_H	T_1	T_2	EM ₁	EM ₂	v_{Ne}	v_{Si}	f_x	L_x
	(1)	(2)	(2)	(3)	(3)	(4)	(4)	(5)	(6)
MV Ori	10.10 ^{0.56} _{0.55}	13.81 ^{0.65} _{0.67}	90.00 ^{0.00} _{19.17}	2.25 ^{0.17} _{0.05}	0.72 ^{0.11} _{0.04}	153 ⁹⁶ ₂₂₇	986 ²⁰² ₆₁	4.6 ^{4.9} _{4.4}	1.1
TU Ori	9.20 ^{1.50} _{1.50}	15.67 ^{2.27} _{1.62}	69.09 ^{13.91} _{16.47}	1.04 ^{0.16} _{0.18}	0.56 ^{0.16} _{0.15}	319 ⁴¹⁰ ₂₂₀	646 ⁴⁸⁴ ₅₉₇	2.6 ^{2.7} _{2.4}	0.6
V2279 Ori	5.43 ^{0.49} _{0.50}	9.18 ^{1.09} _{1.02}	45.61 ^{3.52} _{3.38}	0.93 ^{0.17} _{0.16}	1.50 ^{0.10} _{0.09}	115 ²⁶⁹ ₁₁₅	374 ²⁵⁷ ₁₆₇	4.9 ^{5.1} _{4.7}	1.1
V348 Ori	2.55 ^{0.25} _{0.23}	10.27 ^{0.70} _{0.71}	41.10 ^{1.66} _{1.53}	0.61 ^{0.10} _{0.09}	2.80 ^{0.08} _{0.08}	209 ²⁴ ₉₅	258 ⁹⁸ ₂₅₈	9.4 ^{9.9} _{8.9}	1.9
V1229 Ori	2.76 ^{0.28} _{0.28}	9.61 ^{0.78} _{1.19}	35.15 ^{1.31} _{1.53}	0.56 ^{0.08} _{0.09}	2.47 ^{0.07} _{0.12}	153 ⁵⁸ ₁₂₃	679 ⁴⁵⁵ ₃₈₀	5.7 ^{6.0} _{5.5}	1.2
V1399 Ori	3.14 ^{0.36} _{0.24}	9.70 ^{0.73} _{0.76}	31.33 ^{1.16} _{1.19}	0.62 ^{0.12} _{0.09}	2.20 ^{0.09} _{0.08}	257 ⁶⁴ ₅₀	268 ¹²¹ ₁₈₉	7.3 ^{7.7} _{7.0}	1.5
V2299 Ori	10.58 ^{0.84} _{0.73}	16.83 ^{2.96} _{2.71}	57.82 ^{19.51} _{10.68}	0.81 ^{0.18} _{0.55}	1.23 ^{0.45} _{0.17}	219 ⁸⁵ ₁₀₃	218 ²⁶⁷ ₂₁₈	4.4 ^{4.6} _{4.2}	1.0
LR Ori	4.09 ^{0.82} _{0.74}	12.00 ^{0.87} _{1.55}	60.00 ^{11.00} _{10.53}	0.57 ^{0.13} _{0.14}	0.51 ^{0.25} _{0.03}	213 ¹¹² ₉₉	179 ²²¹ ₁₇₉	1.9 ^{2.0} _{1.8}	0.4
2MASS3	5.10 ^{0.84} _{0.80}	14.46 ^{1.11} _{1.32}	74.60 ^{15.40} _{17.00}	0.36 ^{0.40} _{0.03}	0.57 ^{0.09} _{0.09}	153 ¹²² ₅₀	50 ¹¹² ₃₇₃	1.6 ^{1.7} _{1.5}	0.4
MT Ori	3.38 ^{0.12} _{0.11}	12.35 ^{0.78} _{0.64}	40.95 ^{0.96} _{8.17}	1.37 ^{0.22} _{0.17}	9.96 ^{0.17} _{0.22}	195 ²⁷ ₂₄	289 ⁵⁸ ₈₉	34.5 ^{0.8} _{1.7}	7.2
LU Ori	4.45 ^{0.63} _{0.64}	10.96 ^{0.49} _{0.48}	45.35 ^{4.58} _{3.97}	0.68 ^{0.15} _{0.14}	0.77 ^{0.06} _{0.06}	322 ⁸⁷ ₁₃₄	470 ²¹³ ₁₈₁	2.6 ^{2.7} _{2.4}	0.6
V1333 Ori	9.29 ^{0.58} _{0.60}	12.04 ^{0.61} _{0.75}	30.39 ^{2.57} _{2.60}	1.52 ^{0.25} _{0.27}	1.30 ^{0.20} _{0.15}	222 ⁸⁷ ₂₀₈	636 ⁶³⁵ ₂₆₀	3.3 ^{3.5} _{3.2}	0.7
Par 1842	1.77 ^{0.43} _{0.37}	10.82 ^{0.93} _{1.07}	36.39 ^{2.14} _{2.19}	0.45 ^{0.11} _{0.10}	1.52 ^{0.09} _{0.08}	216 ³¹ ₁₃₈	556 ²⁷⁶ ₃₄₁	4.3 ^{4.5} _{4.1}	0.9
V1330 Ori	4.95 ^{0.45} _{0.40}	10.46 ^{0.74} _{0.47}	43.05 ^{3.08} _{4.95}	0.65 ^{0.13} _{0.11}	1.57 ^{0.07} _{0.08}	152 ¹⁷⁶ ₁₀₈	254 ¹²⁴ ₂₅₃	5.3 ^{5.6} _{5.0}	1.1
Par 1837	5.45 ^{0.37} _{0.84}	7.22 ^{1.44} _{1.49}	45.03 ^{4.66} _{5.42}	0.35 ^{0.21} _{0.09}	0.52 ^{0.06} _{0.04}	321 ¹⁴⁰ ₁₃₈	597 ²⁸⁸ ₃₂₆	1.5 ^{1.6} _{1.4}	0.3
Par 1895	0.05 ^{0.27} _{0.04}	13.13 ^{1.93} _{1.31}	64.33 ^{15.71} _{9.72}	0.18 ^{0.05} _{0.04}	0.39 ^{0.04} _{0.05}	318 ²⁹⁰ ₁₅₆	253 ⁹⁹ ₈₉	1.5 ^{1.5} _{1.4}	0.3
V1279 Ori	2.02 ^{0.58} _{0.40}	9.58 ^{0.92} _{1.08}	38.34 ^{2.67} _{2.52}	0.26 ^{0.10} _{0.07}	0.92 ^{0.05} _{0.07}	279 ⁵⁵ ₁₃₂	247 ¹⁰¹ ₁₉₉	2.7 ^{2.8} _{2.5}	0.5
V491 Ori	16.21 ^{0.91} _{0.50}	—	43.40 ^{2.23} _{3.08}	—	2.69 ^{0.06} _{0.10}	—	400 ³⁵⁸ ₂₂₀	7.7 ^{8.1} _{7.3}	1.8
Par 1839	2.99 ^{0.86} _{0.84}	11.67 ^{1.00} _{1.22}	81.22 ^{8.78} _{11.71}	0.48 ^{0.11} _{0.11}	0.43 ^{0.06} _{0.03}	269 ⁸⁸ ₁₆₄	278 ²⁰⁰ ₂₇₇	1.9 ^{2.0} _{1.8}	0.4
LQ Ori	0.29 ^{0.20} _{0.23}	10.52 ^{0.36} _{0.31}	34.28 ^{2.16} _{1.32}	0.68 ^{0.11} _{0.07}	1.89 ^{0.15} _{0.07}	213 ³¹ ₂₉	221 ¹⁶⁰ ₂₂₀	5.0 ^{5.3} _{4.8}	1.0
V1326 Ori	3.19 ^{0.41} _{0.44}	6.04 ^{0.55} _{0.50}	29.46 ^{1.56} _{1.21}	0.98 ^{0.21} _{0.18}	1.27 ^{0.06} _{0.06}	191 ³⁹ ₅₉	301 ¹⁸⁸ ₁₉₄	2.7 ^{2.8} _{2.6}	0.6
COUP 1023	5.56 ^{1.34} _{1.13}	18.96 ^{3.09} _{2.95}	78.00 ^{12.00} _{14.96}	0.60 ^{0.13} _{0.13}	0.28 ^{0.11} _{0.04}	86 ⁸³ ₇₈	243 ¹⁹³ ₁₄₅	1.7 ^{1.8} _{1.6}	0.4
V495 Ori	5.24 ^{0.72} _{0.69}	11.61 ^{1.47} _{1.01}	69.02 ^{14.58} _{9.43}	0.51 ^{0.12} _{0.11}	0.66 ^{0.06} _{0.07}	257 ¹²⁷ ₁₃₃	307 ¹⁶⁵ ₁₄₃	3.0 ^{3.2} _{2.9}	0.7
V1228 Ori	3.04 ^{0.80} _{1.54}	9.18 ^{0.78} _{0.65}	37.33 ^{5.33} _{2.67}	0.48 ^{0.17} _{0.10}	0.62 ^{0.05} _{0.08}	135 ⁷⁴ ₇₄	359 ⁵⁰ ₃₅₄	1.7 ^{1.8} _{1.6}	0.4
V1501 Ori	3.41 ^{0.82} _{0.69}	12.19 ^{0.99} _{1.29}	42.42 ^{4.09} _{5.42}	0.59 ^{0.18} _{0.15}	0.79 ^{0.11} _{0.07}	301 ¹⁰⁵ ₉₇	384 ¹⁸⁰ ₃₀₇	2.5 ^{2.7} _{2.4}	0.6
V1496 Ori	3.27 ^{0.83} _{0.84}	13.00 ^{2.11} _{1.44}	65.90 ^{18.16} _{10.35}	0.27 ^{0.09} _{0.07}	0.41 ^{0.05} _{0.05}	210 ⁵⁵⁶ ₁₈₆	36 ²⁸⁶ ₃₁	1.6 ^{1.7} _{1.6}	0.4
2MASS1	14.49 ^{0.82} _{0.82}	12.07 ^{1.61} _{1.32}	47.93 ^{9.85} _{6.32}	1.27 ^{0.27} _{0.28}	1.08 ^{0.18} _{0.18}	—	770 ²⁴⁶ ₂₉₃	3.6 ^{3.8} _{3.4}	0.9
COUP 450	30.95 ^{0.78} _{0.78}	—	34.92 ^{1.55} _{1.34}	—	5.58 ^{0.12} _{0.26}	—	460 ⁶⁰³ ₃₀₂	11.2 ^{0.5} _{0.6}	3.3
Par 1936	16.88 ^{1.94} _{1.76}	13.28 ^{1.54} _{1.42}	83.00 ^{7.00} _{7.05}	0.80 ^{0.21} _{0.16}	0.26 ^{0.03} _{0.02}	—	356 ¹⁰⁸⁹ ₃₅₆	1.3 ^{1.4} _{1.2}	0.3
COUP 662	21.52 ^{1.66} _{1.60}	—	89.00 ^{1.00} _{1.00}	0.00 ^{0.00} _{0.00}	0.62 ^{0.02} _{0.02}	—	364 ⁷²⁹ ₃₅₉	2.6 ^{2.7} _{2.5}	0.6
V1398 Ori	5.01 ^{1.05} _{1.24}	12.89 ^{1.31} _{1.00}	79.00 ^{11.00} _{11.05}	0.50 ^{0.12} _{0.16}	0.36 ^{0.06} _{0.06}	197 ¹²¹ ₁₉₅	415 ³¹⁴ ₂₉₀	1.7 ^{1.7} _{1.6}	0.4

NOTE—(1) 10^{21} cm⁻² (2) 10^6 K (3) 10^{54} cm⁻³ (4) km s⁻¹ (5) 10